

LoSA: Long-Short-range Adapter for Scaling End-to-End Temporal Action Localization

Akshita Gupta^{*1,2,3}, Gaurav Mittal^{*1}, Ahmed Magooda¹, Ye Yu¹,
Graham W. Taylor^{2,3}, Mei Chen¹

Microsoft¹ University of Guelph² Vector Institute for AI³

Abstract. Temporal Action Localization (TAL) involves localizing and classifying action snippets in an untrimmed video. The emergence of large video foundation models has led RGB-only video backbones to outperform previous methods needing both RGB and optical flow modalities. Leveraging these large models is often limited to training only the TAL head due to the prohibitively large GPU memory required to adapt the video backbone for TAL. To overcome this limitation, we introduce LoSA, the first memory-and-parameter-efficient backbone adapter designed specifically for TAL to handle untrimmed videos. LoSA specializes for TAL by introducing **L**ong-**S**hort-range **A**dapters that adapt the intermediate layers of the video backbone over different temporal ranges. These adapters run parallel to the video backbone to significantly reduce memory footprint. LoSA also includes Long-Short-range Fusion that strategically combines the output of these adapters from the video backbone layers to enhance the video features provided to the TAL head. Experiments show that LoSA significantly outperforms all existing methods on standard TAL benchmarks, THUMOS-14 and ActivityNet-v1.3, by scaling end-to-end backbone adaptation to billion-parameter-plus models like VideoMAEv2 (ViT-g) and leveraging them beyond head-only transfer learning.

1 Introduction

Temporal Action Localization (TAL) refers to localizing and classifying action snippets in an untrimmed (arbitrarily long) video. TAL is crucial for applications in video indexing/search, surveillance, responsible AI, and robotics [37]. Several methods have emerged for TAL over the years that formulate it as a downstream transfer learning task [28, 34, 39, 44]. Most works [20, 44] perform head-only transfer learning where a frozen video backbone, generally pretrained on a large corpus of trimmed (<30s) videos like Kinetics-600 [6], is employed to extract features from untrimmed videos (Fig. 1a). These features are then concatenated and fed to a trainable head designed to perform TAL. In this context,

* Equal Contribution

This work was done as Akshita’s internship project at Microsoft.

while certain studies [29, 31, 44] have shown improved results using both RGB and optical flow features, advances in video foundation models have enabled recent works [34, 36] to employ models like ViT-g with over 1 B parameters [43] to surpass previous methods with RGB features alone. This is because the effectiveness of data and model scaling is able to offset the need for expensive optical flow estimation (Fig 1e).

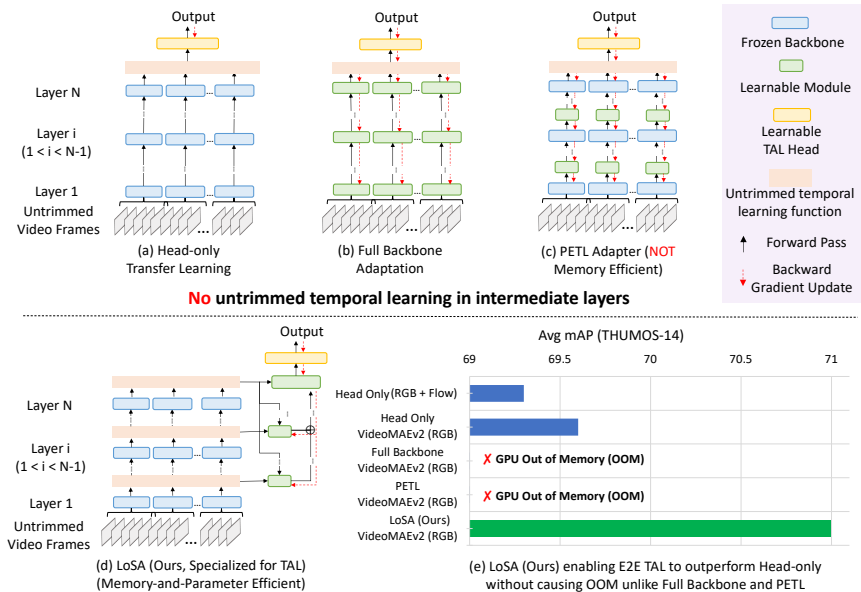


Fig. 1: TAL Training Strategies/Performance. (a) **Head-only Transfer Learning:** Untrimmed video frames processed as independent set of clips by the frozen backbone, features concatenated after last layer, and fed to learnable TAL head. (b) **Full-backbone Transfer Learning:** Untrimmed video frames processed as independent set of clips by a learnable backbone, features concatenated after last layer, and fed to learnable TAL head. (c) **Parameter-Efficient Transfer Learning (PETL):** Untrimmed video frames processed as independent set of clips by a frozen backbone fitted with learnable adapter modules, features concatenated after last layer, and fed to learnable TAL head. Gradients backpropagate through entire backbone making PETL adapters parameter-efficient but not memory efficient. No untrimmed temporal learning in intermediate layers in (a-c). (d) **LoSA (Ours):** Untrimmed video frames processed jointly at each intermediate layer, enabling untrimmed temporal learning by long- and short-range adapters (green) to obtain TAL-enhanced features, and fed to learnable TAL head. No gradient backpropagating through backbone making LoSA both memory and parameter efficient. (e) On VideoMAEv2 (ViT-g) with THUMOS-14, only LoSA (d) can perform end-to-end TAL while full backbone (b) and PETL (c) leads to GPU Out of Memory error, thereby significantly outperforming head-only (a).

Since TAL is performed on untrimmed videos, and these foundation models are typically trained on trimmed videos, there can be a distribution shift between backbone features and the downstream TAL task [38]. This can result

in confusion near action boundaries and fragmented action snippets. This also suggests that adapting the backbone of the video foundation models beyond head-only transfer learning could help to further improve performance. Meanwhile, the massive size of foundation models, along with the long sequence length of untrimmed videos, make backbone adaptation prohibitively expensive w.r.t. GPU memory. Some TAL methods [8, 9, 23, 45] propose memory optimizations to support full backbone adaptation (Fig 1b), but they cannot operate at the scale of foundation models, which are expected to increase in size over time.

More recently, Parameter-efficient Transfer Learning/Fine-Tuning (PETL/PEFT) approaches [16, 17, 30, 42] emerged, motivated by the computational constraints of adapting billion-parameter foundation models for downstream tasks. However, existing approaches do not have a mechanism to adapt the intermediate layers of the base foundation model to handle untrimmed videos (as showing in Fig 1c). These approaches are ill-equipped to work optimally for TAL, since understanding long-range and short-range temporal dependencies is required to correctly localize a wide range of actions.

To overcome this challenge, we introduce LoSA, the first memory- and parameter-efficient backbone adapter that is tailored for TAL and untrimmed videos to harness large video foundation models more effectively beyond head-only transfer learning (Fig 1d). LoSA comprises a series of lightweight Long-range and Short-range Adapters that are attached to the intermediate layers of the video backbone. With video being processed by the large video foundation model as a sequence of trimmed video clips, these adapters learn to adapt the intermediate layers of the video backbone by capturing long-term and short-term dependencies among the video frames respectively. This allows an improved long-range temporal learning of the untrimmed video at each intermediate layer (Fig 1d) while also capturing the fine-grained short-term temporal changes in the video, allowing for more effective localization of actions. To allow each intermediate layer to contribute directly towards improving TAL, the adapters leverage cross-attention between the intermediate layers and the last layer of the video backbone to transform the output of intermediate layers.

The Long-range and Short-range Adapters run parallel to the video backbone and their outputs directly aggregate with the last layer features. This circumvents gradient backpropagation through the video backbone, which significantly reduces the memory footprint of adapting the backbone for TAL. To facilitate this aggregation, LoSA introduces Long-Short-range Fusion with a learnable gating function to weigh the contribution of each intermediate layer and fuse them together with the output of the last layer to generate improved features for the TAL head. These TAL-enhanced features enable more accurate action boundaries compared to head-only transfer learning as evident from the superior performance in Fig 1e.

We demonstrate LoSA’s effectiveness in adapting video backbones for TAL on both transformer-based and CNN-based models including VideoMAEv2 (ViT-g) which has >1 B parameters. Experiments on standard TAL datasets, THUMOS-14 and ActivityNet-v1.3, show that LoSA significantly outperforms all existing

methods and PETL techniques by enabling end-to-end backbone adaptation of large video foundation models beyond head-only transfer learning. In summary:

1. We address the significant challenge in the TAL field of scaling end-to-end training by introducing LoSA, an innovative solution for TAL that is specifically tailored for untrimmed videos.
2. LoSA comprises a novel adapter design to enable memory-and-parameter efficiency for untrimmed videos by employing a series of lightweight Long-range and Short-range adapters that run parallel to the video backbone and a Long-Short-range Fusion module to adaptively fuse the outputs from the adapters to improve TAL.
3. LoSA is capable of end-to-end backbone adaptation of over-billion-parameter video models beyond head-only transfer learning, establishing new SOTA for TAL.

2 Related Work

2.1 Temporal Action Localization (TAL)

Most TAL approaches leverage RGB and optical flow features pre-extracted from a video backbone. Among these are two-stage methods [3, 14, 21, 22, 39, 46], which generate pre-defined action proposals and then classify them into action classes while regressing the actual action boundaries, and one-stage methods [20, 24, 29, 31, 44], which perform TAL in a single pass without separately generating action proposals. These approaches perform head-only transfer learning, treating the video backbone as frozen. In spite of shallow training and leveraging relatively small backbones like I3D [7], TSN [35], and TSP [1], they achieve competitive performance by using optical flow that enhances temporal understanding. However, optical flow estimation is computationally expensive, making it challenging to scale on increasingly large video datasets. Recently, large video foundation models [34, 36] have demonstrated superior performance on TAL using RGB features only. These are also limited to head-only transfer learning due to the prohibitively large GPU memory footprint for end-to-end training.

2.2 Backbone Adaptation approaches for TAL

There exist approaches [8, 9, 23, 45] that attempt to adapt an RGB-only video backbone beyond head-only transfer learning to mitigate the need for optical flow. They do so via memory optimizations such as reducing spatial resolution [23], channel activations [9], feature caching [8], and rewiring the backbone [45]. While they can operate on relatively small backbones like SlowFast-101 [13], ViT-B [12], and ResNet-50 [15], they fail to scale to the size of current visual foundation models with potentially billions of parameters [34]. LoSA, with its memory- and parameter-efficient backbone adapter, mitigates this issue and enables backbone adaptation to leverage RGB-only large video backbones beyond head-only transfer learning to outperform all existing methods.

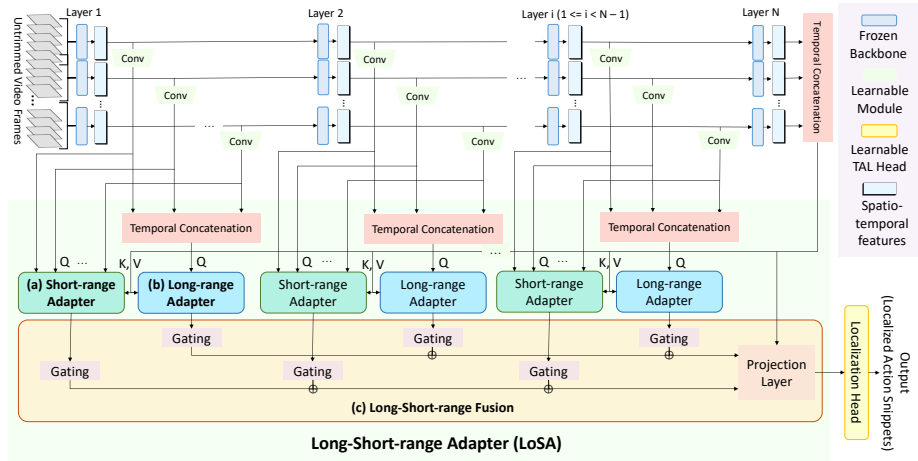


Fig. 2: LoSA Overview: LoSA comprises a series of Long-range and Short-range Adapters that attach to the intermediate layers $1, \dots, N-1$ of a video backbone. (a) Each **Short-range Adapter** consists of a cross-attention module that uses the video clip-level spatio-temporal features of an intermediate layer as Query and the last layer temporally concatenated features as Key and Value. (b) Similarly, each **Long-range Adapter** uses a cross-attention module to cross-attend the temporally concatenated long-range untrimmed video features of an intermediate layer as Query (Q) and the last layer temporally concatenated features as Key (K) and Value (V). (c) Finally, the **Long-Short-range Fusion** module learns scaling parameters to gate the contribution of the Long-range and Short-range Adapters and combines them with the temporally concatenated last layer features via a projection layer to generate the TAL-enhanced features going into the learnable TAL head for outputting the localized action snippets.

2.3 Parameter-efficient Transfer Learning (PETL)

With the advent of large-language models (LLMs) [4, 32], parameter-efficient transfer learning/finetuning (PETL/PEFT) [16, 17] has emerged to reduce computational costs of finetuning LLMs on downstream tasks. Inspired by LLM-based PETL, vision-based PETL was developed to enable efficient transfer learning on visual tasks. Yet, most approaches are parameter-efficient but not memory-efficient [30, 40] as their design causes gradient backpropagation through the backbone. Some more recent methods [11, 30, 41] attempt to address memory efficiency, but no existing method, to the best of our knowledge, is suited to handle untrimmed videos. LoSA is the first memory- and parameter-efficient approach that is designed for TAL.

3 Method

We describe the different components of LoSA in the following subsections, starting with laying out the preliminaries. Fig 2 provides an overview of the model.

3.1 Preliminaries

Let g denote a video backbone comprising N layers, f_1, \dots, f_N , defined as $g = f_N(f_{N-1}(\dots f_1(\mathbf{X}) \dots))$, where \mathbf{X} is the input to the backbone. Let F_i be the feature representation obtained as the output from layer f_i .

To adapt g for TAL, \mathbf{X} is an untrimmed video comprising an arbitrary number of frames. Since the existing video backbones are trained using trimmed video clips, we divide \mathbf{X} into a sequence of T clips x_1, \dots, x_T where each clip is a sequence of T' frames such that $T' \ll$ total number of frames in the untrimmed video. Depending on the stride, the clips can be either overlapping or disjoint. We feed each clip $x_t \forall t \in \{1 \dots T\}$ to the video backbone g to generate a set of feature maps $F_i^{x_t} \forall i \in \{1 \dots N\}, t \in \{1 \dots T\}$ corresponding to all the layers of g . We assume each feature map $F_i^{x_t} \in \mathbb{R}^{T_i \times H_i \times W_i \times C_i}$ where T_i, H_i, W_i , and C_i denote the temporal, height, width, and channel dimensions of the video clip features at intermediate layer f_i . Further, at each intermediate layer f_i , let $\mathbf{F}_i^{\mathbf{X}} = \{F_i^{x_1}, \dots, F_i^{x_T}\} \in \mathbb{R}^{TT_i \times H_i \times W_i \times C_i}$ be the concatenation of the feature maps along the temporal dimension.

3.2 Short-range Temporal Adapter

Let us consider an intermediate spatio-temporal feature map $F_i^{x_t} \in \mathbb{R}^{T_i \times H_i \times W_i \times C_i}$ from layer f_i at temporal location t where $i \in \{1 \dots N - 1\}$ and $t \in \{1 \dots T\}$ obtained from feeding a trimmed video clip of the untrimmed video to the video backbone. Since $T' \ll$ total number of frames in the untrimmed video, $F_i^{x_t}$ captures a short-range temporal context and provides a fine-grained temporal understanding in the local temporal neighborhood of the untrimmed video around its timestamp t . The video backbone processes each $F_i^{x_t} \forall t \in \{1 \dots T\}$ independent of each other, which prevents the context of the full untrimmed video to influence the representation learning. So to perform transfer learning over these features for effective end-to-end action localization, LoSA comprises a series of Short-range Temporal Adapters (Fig 2a) to adapt $F_i^{x_t} \forall t \in \{1 \dots T\}, i \in \{1 \dots N - 1\}$ conditioned on all the short-range spatio-temporal feature maps from the last layer, $F_N^{x_t} \forall t \in \{1 \dots T\}$.

For this, we introduce a multi-headed cross-attention module in the Short-range Temporal Adapter at each intermediate layer $f_i \forall i \in \{1 \dots N - 1\}$ of the video backbone. We first employ a convolutional block at each layer $i \in \{1 \dots N\}$ of the video backbone to process the spatial dimensions by transforming $F_i^{x_t} \in \mathbb{R}^{T_i \times H_i \times W_i \times C_i} \rightarrow F'_i{}^{x_t} \in \mathbb{R}^{T_i \times C_i}$. We then feed $F'_i{}^{x_t}$ as Query and $\mathbf{F}'_N{}^{\mathbf{X}}$ as Key and Value to the cross-attention module, where $\mathbf{F}'_N{}^{\mathbf{X}} = \{F'_N{}^{x_1}, \dots, F'_N{}^{x_T}\}$ is the concatenation of the transformed feature maps from last layer N of the video backbone along the temporal dimension. The cross-attention module outputs $FS_i^{x_t} \in \mathbb{R}^{T_i \times C_i} \forall t \in \{1 \dots T\}, i \in \{1 \dots N - 1\}$, representing the short-range features adapted for end-to-end TAL.

3.3 Long-range Temporal Adapter

While the Short-range Temporal Adapters enable features from trimmed video clips to be adapted at each temporal location for TAL for all intermediate layers, it is not sufficient for effectively localizing actions. Understanding the long-range temporal relationship among frames over the full untrimmed video is required to correctly identify the action boundaries and effectively distinguish between foreground and background. No existing method, including both full backbone adaptation and PETL (Fig 1b,c), incorporate a mechanism to capture this long-range temporal understanding in an untrimmed video directly at intermediate layers. To address this, LoSA comprises a series of Long-range Temporal Adapters (Fig 2b) that learn to adapt the full temporally concatenated feature map sequence $\mathbf{F}_i^{\mathbf{X}}$ jointly for end-to-end TAL at each intermediate layer $f_i \forall i \in \{1 \dots N - 1\}$.

Similar to the Short-range Temporal Adapters, the Long-range Temporal Adapter adapts the feature map sequence at a given intermediate layer conditioned on the feature map sequence from the last layer of the video backbone. For this, each Long-range Temporal Adapter consists of a cross-attention module at each intermediate layer $f_i \forall i \in \{1 \dots N - 1\}$ of the video backbone. We feed the output of the convolutional block, concatenated along temporal dimension, $\mathbf{F}'_i^{\mathbf{X}}$ as Query and $\mathbf{F}'_N^{\mathbf{X}}$ as Key and Value to the cross-attention module. By doing so, we consider the last layer features as reference to cross-attend the intermediate long-range temporal features to adapt the latter into what directly improves the features going into TAL. The cross-attention module outputs $\mathbf{FL}_i^{\mathbf{X}} \in \mathbb{R}^{Tt_i \times C_i} \forall i \in \{1 \dots N - 1\}$, representing the long-range features adapted for end-to-end TAL.

3.4 Long-Short-range Fusion

The output of the adapters comprises feature representations at different temporal ranges and different intermediate layers of the video backbone. We maintain that these features from intermediate layers should function to enhance the temporal understanding of the last layer features during end-to-end training. We therefore need to strategically fuse these representations to generate TAL-enhanced feature representations for the TAL head that are the most optimal in localizing actions.

For this, after obtaining the short-range and long-range features from each intermediate layer, we introduce a Long-Short-range Fusion module (Fig 2c) to learn to strategically fuse these features along with the last layer features to obtain the TAL-enhanced features that are fed to the TAL head. As shown in Fig 2c, the Long-Short-range Fusion module comprises a short-range gating layer, $\text{Gate}_i^{\text{sh}}$, at each intermediate layer f_1, \dots, f_{N-1} . $\text{Gate}_i^{\text{sh}}$ multiplies the temporally concatenated short-range features, obtained from the Short-range Adapter, at layer f_i , $\mathbf{FS}_i^{\mathbf{X}} = \{FS_i^{x_1}, \dots, FS_i^{x_T}\} \in \mathbb{R}^{Tt_i \times C_i}$ with a learnable scaling parameter p_i^{sh} to compute the short-range contribution at intermediate layer f_i as, $\text{Gate}_i^{\text{sh}}(\mathbf{FS}_i^{\mathbf{X}}) = p_i^{\text{sh}}\mathbf{FS}_i^{\mathbf{X}}$. Next, we sum the short-range contributions over all

intermediate layers as, $\mathbf{FS}^{\mathbf{X}} = \sum_{i=1}^{N-1} \text{Gate}_i^{\text{sh}}(\mathbf{FS}_i^{\mathbf{X}})$. We note that depending on the network architecture T_i may vary in size across intermediate layers. To accommodate that and facilitate fusion, we use linear projection layers, as needed, to transform each $T_i \rightarrow T_N$, temporal dimension of the last layer f_N .

Similarly, the Long-Short-range Fusion module comprises a long-range gating layer, $\text{Gate}_i^{\text{lo}}$, at each intermediate layer f_1, \dots, f_{N-1} . $\text{Gate}_i^{\text{lo}}$ multiplies the long-range features, obtained from the Long-range Adapter, at layer f_i , $\mathbf{FL}_i^{\mathbf{X}} \in \mathbb{R}^{T_i \times C_i} \forall i \in \{1 \dots N-1\}$ with a learnable scaling parameter p_i^{lo} to compute the long-range contribution at intermediate layer f_i as, $\text{Gate}_i^{\text{lo}}(\mathbf{FL}_i^{\mathbf{X}}) = p_i^{\text{lo}} \mathbf{FL}_i^{\mathbf{X}}$. Next, we sum the long-range contributions over all intermediate layers as, $\mathbf{FL}^{\mathbf{X}} = \sum_{i=1}^{N-1} \text{Gate}_i^{\text{lo}}(\mathbf{FL}_i^{\mathbf{X}})$. Similar to short-range gating, we use linear projection layers, as needed, to make temporal dimensions at different layers consistent with that of last layer f_N , *i.e.*, T_N .

After obtaining $\mathbf{FS}^{\mathbf{X}}$ and $\mathbf{FL}^{\mathbf{X}}$, we combine them with the last layer features $\mathbf{F}_N^{\mathbf{X}}$ by addition and finally feed the concatenation of the resulting set of features to a linear projection layer $\text{Proj}: \mathbb{R}^{T_N \times 2C} \rightarrow \mathbb{R}^{T_N \times C}$ to obtain the TAL-enhanced features, $\mathbf{FT}_N^{\mathbf{X}}$, to be fed to the TAL head as,

$$\mathbf{FS}'^{\mathbf{X}} = \mathbf{FS}^{\mathbf{X}} + \mathbf{F}_N^{\mathbf{X}}, \quad \mathbf{FL}'^{\mathbf{X}} = \mathbf{FL}^{\mathbf{X}} + \mathbf{F}_N^{\mathbf{X}}, \quad (1)$$

$$\mathbf{FT}_N^{\mathbf{X}} = \text{Proj}([\mathbf{FS}'^{\mathbf{X}}, \mathbf{FL}'^{\mathbf{X}}]). \quad (2)$$

By doing so, we consider the short-range and long-range contribution of intermediate layers as a residual contribution to the original last layer features. In order to mathematically enforce that, we perform zero initialization on the scaling parameters $\{p_i^{\text{sp}}\}_{i=0}^{N-1}$ and $\{p_i^{\text{tem}}\}_{i=0}^{N-1}$ of the gating layers $\{\text{Gate}_i^{\text{sp}}\}_{i=0}^{N-1}$ and $\{\text{Gate}_i^{\text{tem}}\}_{i=0}^{N-1}$ respectively. This ensures that when training starts, the TAL-enhanced features going into the TAL head are effectively the last layer’s original features, providing a stable baseline for leveraging the video backbone g . We finally feed $\mathbf{FT}_N^{\mathbf{X}}$ to the TAL head for generating the localized action snippets as output (Fig 2, bottom-right).

3.5 Enabling Memory-and-Parameter Efficiency

The unique adapter design of LoSA enables temporal video understanding over the full untrimmed video at each intermediate layer of the video backbone during end-to-end training (Fig 1d). This allows the video backbone, originally trained on trimmed videos, to improve its understanding of the untrimmed video over long-range and short-range temporal context. This is unlike any existing end-to-end TAL method, including both full backbone adaptation and PETL (Fig 1b,c), where there is no mechanism to capture this long-range and short-range temporal understanding of an untrimmed video directly at intermediate layers. A crucial challenge in enabling untrimmed temporal learning at each intermediate layer during end-to-end training is the prohibitively large GPU memory footprint. This is because for TAL, each untrimmed video sample in a training batch involves

processing several video clips together. Furthermore, the memory issue is aggravated when leveraging large billion-parameter-plus video backbones. LoSA’s adapter design, performing cross-attention with last layer features, allows the Long-range and Short-range Temporal Adapters to run parallel to the video backbone (as shown in Fig 2). This makes the design memory-and-parameter efficient and circumvents backpropagating gradients through the video backbone, thereby significantly reducing the GPU memory footprint.

4 Experiments

Datasets. We evaluate LoSA on the two standard datasets for TAL: THUMOS-14 [18] and ActivityNet-v1.3 [5]. THUMOS-14 has 20 action classes. Following existing methods [20, 34, 44], we use the 200 untrimmed videos in the validation set for training and test on a set of 212 test videos. ActivityNet-v1.3 has 200 action classes. We use the 10,024 videos from the training set for training and use the 4,926 videos from the validation set for testing.

Model Backbones. We consider three video backbones: SlowFast-101 [13], VideoMAEv2 (ViT-Base) [34], and VideoMAEv2 (ViT-g) [34]. VideoMAEv2 (ViT-g) has ~ 1.01 billion parameters and is one of the more recent large video foundation models. It achieves SOTA performance on several video benchmarks including TAL. We select VideoMAEv2 (ViT-g) in order to demonstrate the scaling limitations of existing methods as well as LoSA’s effectiveness in overcoming those limitations. We select SlowFast-101 and VideoMAEv2 (ViT-Base) as these models (along with others of similar sizes) are widely used in the TAL literature. Moreover, it also helps to evaluate the effectiveness of LoSA on different families of model architecture with SlowFast-101 being CNN-based [19] and VideoMAEv2 (ViT-Base) being a Transformer [33]-based model.

Implementation Details. We train LoSA feeding RGB-frames (similar to existing end-to-end TAL methods) as input to the different video backbones with an initial learning rate of $1e-4$ for THUMOS-14 and $1e-3$ for ActivityNet using a cosine annealing, warmup of 5 epochs, and AdamW [26] optimizer. We use Actionformer as the TAL head with max sequence length of 576 frames at 224×224 spatial resolution with $T' = 16$ frames. We use temporally-consistent spatial augmentation involving random resizing and cropping and autoaugment [10]. We attach Short-range and Long-range Adapters to all the intermediate layers with $n_{\text{heads}} = 4$.

Please refer to the supplementary for additional details.

4.1 Comparison of Head-only vs. End-to-End TAL Training

Table 1 provides a comparison of LoSA with different training strategies available for TAL (as shown in Fig 1). We experiment using THUMOS-14 on SlowFast-101 and VideoMAEv2 (ViT-g) to show the comparison on backbones with sizes

Method	Backbone	End-to-End Adaptation	GPU	Avg mAP (\uparrow)
Head-only	SlowFast-101	✗	1.8 GB	55.1
Full Backbone		✓	14 GB	56.4
LoSA		✓	3.5 GB	58.2
Head-only	VideoMAEv2 (ViT-g)	✗	2.4 GB	69.6
Full Backbone		✓	OOM	-
LoSA		✓	40.6 GB	71.0

Table 1: Comparison of LoSA with other TAL training strategies for TAL on THUMOS-14. E2E Adaptation is ✓ when backbone adaptation (end-to-end training) happens along with learning the TAL head. GPU - peak GPU memory occupied overall by training for batch size of 1 on an A100 GPU. OOM - out of GPU memory error when even batch size of 1 cannot fit in GPU. Avg mAP is ‘-’ when there is OOM as training fails to run. On 1.01B parameter VideoMAEv2 (ViT-g), only LoSA, by being both memory and parameter efficient, is able to perform end-to-end backbone adaptation beyond Head-only and achieve superior Avg mAP. On SlowFast-101, LoSA can outperform all TAL training strategies.

at different orders of magnitude. We can observe that for both backbones, LoSA significantly outperforms head-only transfer learning (Fig 1a) by 3.1% and 1.4% respectively on Avg mAP. LoSA also outperforms full backbone adaptation on SlowFast-101 by 1.8% Avg mAP. Full backbone adaption (Fig 1b) results in GPU Out of Memory error (OOM) on VideoMAEv2 (ViT-g) owing to the backbone having 1.02 billion parameters, which prevents even a batch size of one training sample to fit in an A100 GPU.

Method	Backbone	End-to-End Adaptation	Backbone Parameters		GPU	Avg mAP (\uparrow)
			Full	Learnable		
Full Backbone	SlowFast-101	✓		62M	14 GB	56.4
ST-Adapter* [27]		✓		8M (-87%)	10 GB	53.2
AIM* [40]		✓	62M	10M (-83%)	12 GB	54.0
UniPT* [11]		✓		13M (-79%)	4.9 GB	56.8
LoSA		✓		12M (-80%)	3.5 GB	58.2
Full Backbone	VideoMAEv2 (ViT-g)	✓		1012M	OOM	-
ST-Adapter* [27]		✓		88M (-91%)	OOM	-
AIM* [40]		✓	1012M	92M (-90%)	OOM	-
UniPT* [11]		✓		115M (-88%)	51.6 GB	66.2
LoSA		✓		143M (-86%)	40.6 GB	71.0

Table 2: Comparison of LoSA with other training strategies for TAL on THUMOS-14. E2E Adaptation is ✓ when backbone adaptation (end-to-end training) happens along with learning the TAL head. GPU - peak GPU memory occupied overall by training for batch size of 1 on an A100 GPU. OOM - out of GPU memory error when even batch size of 1 cannot fit in GPU. Avg mAP is ‘-’ when there is OOM as training fails to run. Learnable column includes percentage reduction in parameters w.r.t. Full column in parentheses. On 1.01 billion parameter VideoMAEv2 (ViT-g), only LoSA, by being both memory and parameter efficient, is able to perform end-to-end backbone adaptation and achieve superior Avg mAP. On SlowFast-101, where all training strategies can operate, LoSA can still outperform all the baselines. *Repurposed for TAL.

4.2 Comparison of different Adapter designs for TAL

Since there exists no previous adapter-based PETL method for TAL, we re-purpose some of the existing PETL approaches to work for TAL using publicly

available implementations. We consider ST-Adapter, AIM, and UniPT for comparison. For SlowFast-101, LoSA significantly outperforms all existing adapter-based methods by at least 1.4% Avg mAP, highlighting the importance of the design of LoSA’s Long-Short-range Adapter tailored specifically for TAL. On VideoMAEv2 (ViT-g), the original implementation of ST-Adapter and AIM leads to an OOM error because, as Table 2 and Fig 1c show, while their learnable parameter count is significantly less than the full backbone, they are not memory efficient, making them unscalable to billion parameter models like VideoMAEv2 (ViT-g). LoSA works on VideoMAEv2 (ViT-g) because it is both memory and parameter efficient. UniPT has a memory-efficient adapter design, allowing it to operate within the GPU memory limit. Meanwhile, LoSA significantly outperforms UniPT as our adapter design to capture temporal context over different temporal ranges specializes the method for TAL and untrimmed videos.

Method	Backbone		Flow	GPU (GB)	mAP					Avg. mAP (†)
	Type	E2E Adaptation			0.3	0.4	0.5	0.6	0.7	
AFSD-RGB [20]	I3D	✗	✗	-	57.7	52.8	45.4	34.9	22.0	43.6
G-TAD [39]	TSN	✗	✓	-	54.5	47.6	40.3	30.8	23.4	39.3
TadTR [24]	I3D	✗	✓	-	62.4	57.4	49.2	37.8	26.3	46.6
AFSD [20]	I3D	✗	✓	-	67.3	62.4	55.5	43.7	31.1	52.0
ActionFormer [44]	I3D	✗	✓	-	82.1	77.8	71.0	59.4	43.9	66.8
Tridet [29]	I3D	✗	✓	-	83.6	80.1	72.9	62.4	47.4	69.3
E2E-TAD [23]	SlowFast-101	✓	✗	14	71.4	66.6	59.4	48.1	36.8	56.4
TALLFormer [8]	VSwin-Base [25]	✓	✗	29	76.0	-	63.2	-	34.5	-
Re ² TAL [45]	Re ² VideoSwin-T	✓	✗	6.8	77.0	71.5	62.4	49.7	36.3	59.4
Re ² TAL [45]	Re ² SlowFast-101	✓	✗	6.8	77.4	72.6	64.9	53.7	39.0	61.5
TadTR [24]	SlowFast-101	✗	✗	-	70.4	66.4	58.3	46.8	33.5	55.1
LoSA (Ours)	SlowFast-101	✓	✗	3.5	74.2	69.3	61.2	49.6	36.3	58.2 _{†3.1}
ActionFormer [34]	VideoMAEv2 (ViT-Base)	✗	✗	-	80.8	75.6	68.3	59.0	45.6	65.9
LoSA (Ours)	VideoMAEv2 (ViT-Base)	✓	✗	6.5	81.1	77.0	70.2	61.1	46.9	67.3 _{†1.4}
ActionFormer [34]	VideoMAEv2 (ViT-g)	✗	✗	-	84.0	79.6	73.0	63.5	47.7	69.6
LoSA (Ours)	VideoMAEv2 (ViT-g)	✓	✗	40.6	85.0	81.1	74.5	65.1	49.3	71.0 _{†1.4}

(a)

Method	Backbone		Flow	GPU (GB)	mAP			Avg. mAP (†)
	Type	E2E Adaptation			0.5	0.75	0.95	
AFSD-RGB [20]	I3D	✗	✗	-	-	-	-	32.9
G-TAD [39]	TSN	✗	✓	-	50.4	34.6	9.0	34.1
TadTR [24]	I3D	✗	✓	-	49.1	32.6	8.5	32.3
AFSD [20]	I3D	✗	✓	-	52.4	35.3	6.5	34.4
ActionFormer [44]	I3D	✗	✓	-	53.5	36.2	8.2	35.6
Tridet [29]	R(2+1)D	✗	✓	-	54.7	38.0	8.4	36.8
E2E-TAD [23]	SlowFast-50	✓	✗	14	50.5	36.0	10.8	35.1
TALLFormer [8]	VSwin-Base [25]	✓	✗	29	54.1	36.2	7.9	35.6
Re ² TAL [45]	Re ² VideoSwin-T	✓	✗	6.8	54.75	37.81	9.03	36.8
Re ² TAL [45]	Re ² SlowFast-101	✓	✗	6.8	55.3	37.9	9.1	37.0
ActionFormer [34]	VideoMAEv2 (ViT-Base)	✗	✗	-	56.5	37.8	7.7	36.8
LoSA (Ours)	VideoMAEv2 (ViT-Base)	✓	✗	6.5	57.7	38.6	8.1	38.1 _{†1.3}
ActionFormer [34]	VideoMAEv2 (ViT-g)	✗	✗	-	57.2	38.3	5.8	37.1
LoSA (Ours)	VideoMAEv2 (ViT-g)	✓	✗	40.6	58.5	39.8	7.8	38.6 _{†1.5}

(b)

Table 3: Temporal action localization performance comparison of LoSA with state-of-the-art methods on (a) **THUMOS-14** and (b) **ActivityNet-v1.3**. E2E Adaptation is ✓ when backbone adaptation (end-to-end training) happens along with learning the TAL head. Flow is ✓ when optical flow features are used. GPU represents peak GPU memory in GBs occupied for training for batch size of 1 on an A100 GPU. GPU is ‘-’ when the backbone is frozen (*i.e.* E2E Adaptation is ✗). LoSA can significantly outperform all existing methods including those using both RGB and Flow as well as performing backbone adaptation for TAL.

4.3 Comparison with State-of-the-Art

We compare LoSA on THUMOS-14 and ActivityNet-v1.3 with existing TAL methods in Tables 3a and 3b. Given the diversity of different setups in previous approaches, we include columns mentioning the video backbone used, whether the method uses optical flow features, and whether the training involves head-only transfer learning (\times in E2E Adaptation column) or backbone adaptation/end-to-end training (\checkmark in E2E Adaptation column). We also include a column to provide the peak GPU memory utilization of adapting the backbone during training with a batch size of 1 on an A100 GPU (for head-only with no backbone adaptation, we report it as -).

As per Table 3a, we can observe that LoSA significantly outperforms head-only training (\times in E2E Adaptation column) on both CNN-based and transformer-based video backbones – SlowFast-101, VideoMAEv2 (ViT-B), and VideoMAEv2 (ViT-g), by 3.1%, 1.4%, and 1.4% on Avg mAP respectively. Similarly in Table 3b, we can see that LoSA outperforms head-only transfer learning on all the video backbones – VideoMAEv2 (ViT-B) and VideoMAEv2 (ViT-g), by 1.3% and 1.5% on Avg mAP respectively. This shows the effectiveness of LoSA in better leveraging and adapting video backbones across different sizes for TAL beyond head-only transfer learning. By doing so, LoSA outperforms all existing TAL methods, including those that use both RGB and optical flow features and those that attempt backbone adaptation, thereby establishing a new SOTA on both THUMOS-14 and ActivityNet-v1.3.

Setup	Avg mAP	Gating Strategy	Avg mAP	Intermediate Layers Avg	
				(f_i)	mAP
LoSA w/o Long-range Adapter	69.1	Gating w/ random initialization	69.1	f_1, \dots, f_{20}	44.4
LoSA w/o Short-range Adapter	69.2	Gating w/ one initialization	68.4	f_{21}, \dots, f_{39}	70.6
LoSA w/o Long-Short-range Fusion	67.8	Cosine similarity scaling	70.0	f_{10}, \dots, f_{30}	69.4
LoSA	71.0	Gating w/ zero initialization (Ours)	71.0	f_{30}, \dots, f_{39}	69.9
				$f_{15}, \dots, f_{20}, f_{35}, \dots, f_{39}$	68.9
				f_1, \dots, f_{39} (All, Ours)	71.0

(a)

(b)

(c)

Table 4: (a) Ablation showing the effectiveness of each component of LoSA. (b) Comparison with different gating strategies showing the significance of doing zero initialization for achieving the best Avg mAP. (c) Analysis on attaching spatial and temporal adapters to different sets of intermediate layers. All experiments in (a-c) performed on THUMOS-14 using VideoMAEv2 (ViT-g).

4.4 Ablation

We conduct an ablation study using THUMOS-14 and VideoMAEv2 (ViT-g), as shown in Table 4a, to highlight the effectiveness of each integral component of LoSA. The table shows that omitting the Long-range or Short-range Adapter reduces Avg mAP by at least 1.8%, indicating the necessity of both in incorporating temporal information at different ranges from the intermediate layers for optimal TAL performance. Next, we conduct an ablation where we remove the Long-Short-range Fusion module and replace it with a simple addition of the

features. As Row 3 in Table 4a shows, removing the Long-Short-range Fusion module leads to a significant drop of 3.2% in Avg mAP. This shows that along with adapting the long-range and short-range temporal information via the respective adapters, it is also critical to learn how to scale the contribution across the intermediate layers to allow the most relevant long-range and short-range temporal information to be incorporated into the features being fed to the TAL head.

4.5 Discussion

Gating w/ zero initialization outperforms all other gating strategies.

In comparing LoSA’s gating layer strategy with alternatives, our focus is on its unique design and efficiency. As detailed in Sec 3.4, we enforce a zero initialization on the scaling parameter in the long-range and short-range gating layers to enable the long-range and short-range contributions to function as a residual contribution with respect to the last layer features. Table 4b shows that this approach yields the highest Avg mAP, outperforming random or one-value initializations. An alternative to parameterized scaling in the gating layer can be to weigh the long-range and short-range contribution of each intermediate layer based on cosine similarity between intermediate features and the last layer features. We find this design also falls short of the gating layer strategy of LoSA. We believe this is because cosine similarity imposes a similarity prior on the scaling parameter, which restricts its ability in scaling the contribution.

Gating parameter learns different values over intermediate layers.

Since the scaling parameter in the long-range and short-range gating layers is a learnable parameter, we assess the distribution of the values learned by the scaling parameter post-training across the intermediate layers of the video backbone. For VideoMAEv2 (ViT-g) on THUMOS-14, we find that the range of learnable parameter values to be $[-0.01, 0.52]$ across the long-range and short-range gating in the intermediate layers. This validates two hypotheses. One, all learnable parameters do not collapse trivially to their originally initialized value of 0. At least some of them learn a non-zero value to scale and provide a meaningful residual contribution from the intermediate layers to the TAL-enhanced features, \mathbf{FT}_N^X , going into the TAL head. Two, the learnable parameters exhibit a range of values which indicates that the scaling parameters learns to contribute differently from the intermediate layers as per their importance in improving the TAL-enhanced features, \mathbf{FT}_N^X .

Effect of adapting different intermediate layers. Our experiments with VideoMAEv2 (ViT-g) on THUMOS-14 reveal that attaching Long-range and Short-range Adapters to all 40 transformer layers yields the highest Avg mAP (see Table 4c), underscoring the contribution of each layer’s temporal information over different time spans to the TAL head in enhancing localization performance. We can also observe that with the deeper half of layers, f_{21}, \dots, f_{39} , we get very close to optimal Avg mAP while shallower half of layers, f_1, \dots, f_{20} ,

leads to low Avg mAP. We believe this is due to deeper layers capturing more comprehensive information about the video than shallower layers. While a combination of all layers is optimal, using only the deeper half of layers can suffice when training resources are even more limited.

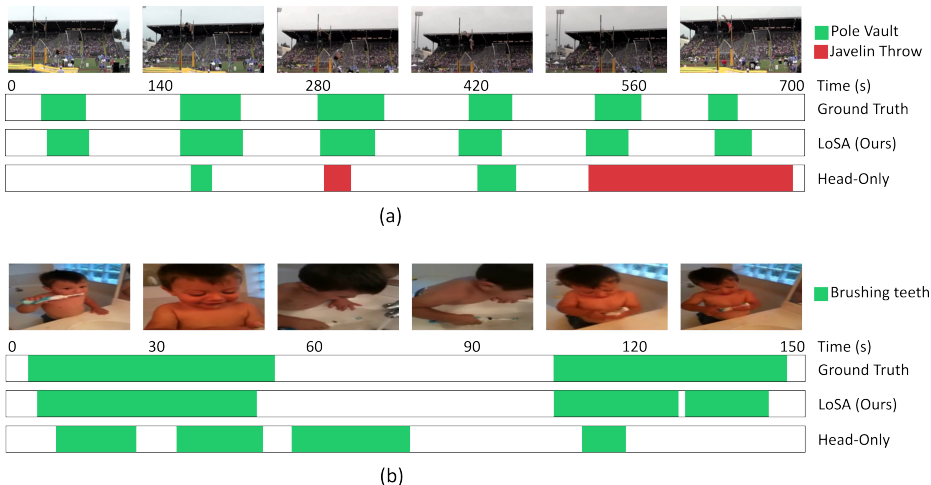


Fig. 3: Qualitative comparison of LoSA with baseline (Head-only) on (a) THUMOS-14 and (b) ActivityNet-v1.3 videos using VideoMAEv2 (ViT-g) showing more accurate action snippets obtained by LoSA.

Visualizations. We conduct a qualitative analysis of the TAL performance on VideoMAEv2 (ViT-g). As shown in Table 1 and 2, only Head-only (Fig 1a) and LoSA (Fig 1d) can work on VideoMAEv2 (ViT-g) without causing GPU OOM error. Fig 3 therefore shows a qualitative comparison of LoSA with head-only transfer learning baseline on THUMOS-14 (Fig 3a) and ActivityNet-v1.3 (Fig 3b).

The figure demonstrates the superior temporal action localization capabilities of LoSA over a conventional head-only transfer learning. The model’s predictions closely match the ground truth, particularly in delineating the nuanced temporal boundaries of the “Pole Vault”, “Hammer Throw”, and “Brushing Teeth” activities. In contrast, the head-only model exhibits clear inaccuracies. These visualizations succinctly demonstrate LoSA’s enhanced precision in TAL with untrimmed videos by introducing an adapter design for end-to-end TAL which can enable temporal understanding over different temporal ranges directly at intermediate layers.

5 Conclusion

We introduce LoSA, the first memory-and-parameter-efficient backbone adapter designed specifically for TAL. LoSA comprises a novel design of Long-range and Short-range Temporal Adapters that are attached to the intermediate layers to

adapt them towards improving TAL, and run parallel to the video backbone to reduce memory footprint. Finally, Long-Short-range Fusion module takes the output from these adapters to fuse and give TAL-enhanced features. This allows LoSA to scale end-to-end backbone adaptation to billion-parameter-plus backbones like VideoMAEv2 (ViT-g) and leverage them beyond head-only training to significantly outperform all existing TAL methods. Our work is the first to go beyond traditional techniques, including full model adaptation and head-only transfer learning, in addressing the challenging problem of adapting video backbones for end-to-end TAL, and proves effective in leveraging large foundation models for performing action localization in untrimmed videos.

6 Acknowledgment

Resources used in preparing this research were provided by Microsoft, and, in part, by the Province of Ontario, the Government of Canada through CIFAR, and [partners of the Vector Institute](#).

Appendix

In this document, we provide additional analysis and details for our work LoSA. Section S1 provides qualitative analysis of LoSA by visualizing and comparing the action snippets localized in the videos. Section S2 provides error analysis of LoSA to highlight additional aspects of the method. Finally, Section S3 expands on the limitations and future work of the LoSA.

S1 Visualizations

In Fig S1, we provide additional visualizations of the action snippets localized by LoSA compared to the baseline of head-only transfer learning in videos from THUMOS-14 using VideoMAEv2 (ViT-g). We can observe that across all the visualizations (Fig S1a-d), LoSA is able to localize action snippets with action boundaries significantly closer to the ground truth than the baseline while also predicting the action class for the snippets more accurately than the baseline. Fig S1a shows a video of “Basketball Dunk”. We can observe that, compared to head-only, LoSA is able to localize the action boundaries for “Basketball Dunk” more precisely with respect to the ground truth. We believe this is due to LoSA’s ability to induce untrimmed temporal video understanding at different temporal ranges in the intermediate layers via the long-range and short-range adapters. This enhances the informativeness of the adapted features of the intermediate layers, contributing towards directly improving TAL and allows to make fine distinctions between foreground and background around action boundaries. This effect is further visible around 160s, where LoSA correctly predicts the snippet action but head-only, due to insufficient temporal context, misclassifies the action as “Volleyball Spiking”, which has similar temporal motion as “Basketball Dunk”.

In Fig S2, we provide visualizations of the action snippets localized by LoSA compared to the baseline of head-only transfer learning in videos from ActivityNet-v1.3 using VideoMAEv2 (ViT-g). We can observe that across all the visualizations (Fig S2a-d), LoSA is able to localize action snippets with action boundaries significantly closer to the ground truth than the baseline. In Fig S2a, where the video shows a kid playing Hopscotch, while the baseline misses the action between 16-24s (false negative) and incorrectly predicts the background as action between 32-40s (false positive), LoSA is able to mitigate both false negative and false positive and accurately predict the start and end timestamps of the action. We believe that this is due to LoSA’s ability to induce untrimmed temporal video understanding at different temporal ranges in the intermediate layers via the long-range and short-range adapters. This improves the adapted feature sequence at each intermediate layer with respect to TAL, allowing the TAL head to perform better action localization.



Fig. S1: Visualizations of LoSA vs. baseline (Head-only Transfer Learning) for THUMOS-14 on VideoMAEv2 (ViT-g). Across all the visualizations (a-d), LoSA is able to localize action snippets (in green) with action boundaries significantly closer to the ground truth than the baseline, leading to fewer false positives and false negatives. LoSA also predicts the action class for the snippets more accurately than the baseline (seen by incorrect class predictions in red by the baseline in (a) and (c)).

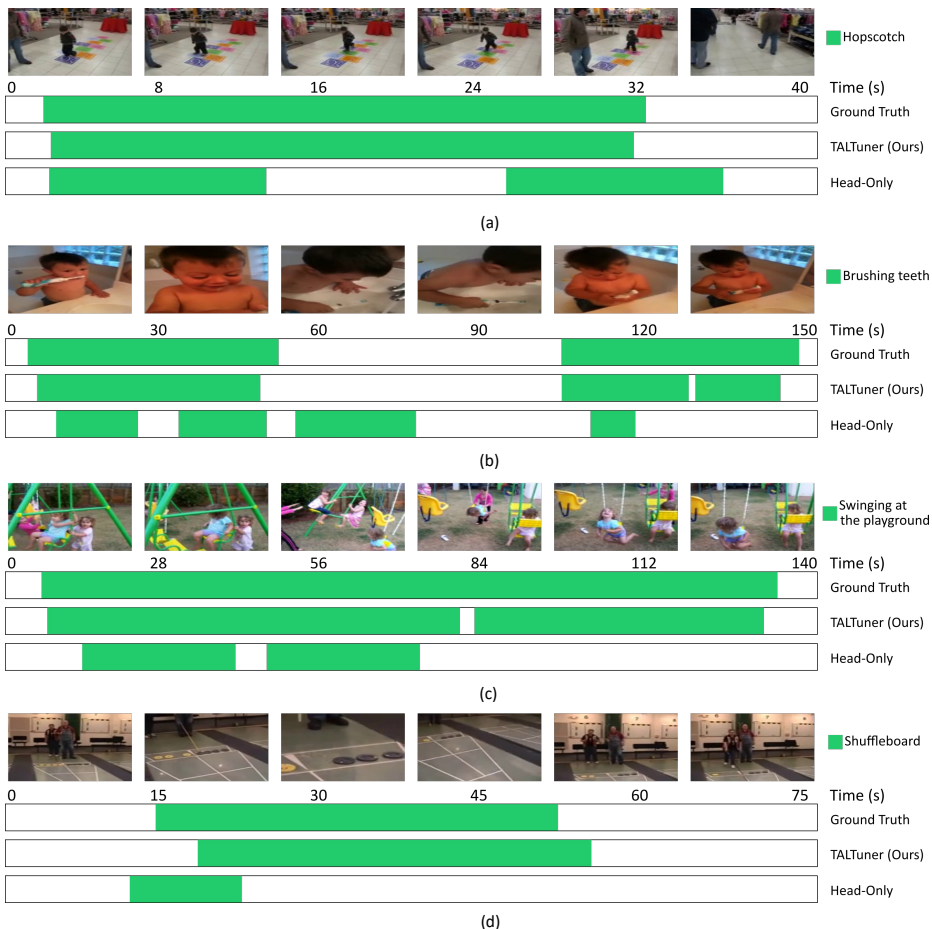


Fig. S2: Visualizations of LoSA vs. baseline (Head-only Transfer Learning) for ActivityNet-v1.3 on VideoMAEv2 (ViT-g). Across all the visualizations (a-d), LoSA is able to localize action snippets (in green) with action boundaries significantly closer to the ground truth than the baseline, leading to fewer false positives and false negatives.

S2 Additional Analysis

In Fig S3, we conduct sensitivity analysis for THUMOS-14 using VideoMAEv2 (ViT-g). This chart takes into consideration coverage, length and number of instances. Coverage presents the relative length of actions compared to the whole video and is further categorized into five bins: Extra Small (XS: (0, 0.02]), Small (S: (0.02, 0.04]), Medium (M: (0.04, 0.06]), Large (L:(0.06, 0.08]), and Extra Large (XL: (0.08, 1.0]). Length presents the actual length of actions and is further divided into five groups: Extra Small (XS: (0, 3]), Small (S: (3, 6]), Medium (M: (6, 12]), Long (L: (12, 18]), and Extra Long (XL: > 18). Finally, number of instances of same class in a video are divided into four parts: Extra Small (XS: 1); Small (S: [2, 40]); Medium (M: [40, 80]); Large (L: > 80). In Fig S3, we show comparison between the baseline, LoSA w/o Long-Short-range Adapter (*the top row*) and our method LoSA (*the bottom row*). We can observe that the performance for both XS and XL improves significantly with our method LoSA compared to the baseline, LoSA w/o Long-Short-range Adapter. We believe this is because by having the untrimmed temporal learning at different temporal ranges in the intermediate layers via the long-range and short-range temporal adapters, LoSA is able to capture complex scene details required for long action instances as well as fine-grained information required for shorter duration actions respectively.

In Fig S4, we conduct a False Positive (FP) analysis at tIoU=0.5 for THUMOS-14 using VideoMAEv2 (ViT-g). Similar to Fig S3, we show comparison between the baseline, LoSA w/o Long-Short-range Adapter (Fig S4a) and our method LoSA (Fig S4b). We can see a drop in the wrong label prediction error with LoSA compared to LoSA w/o Long-Short-range Adapter. This shows the significance of incorporating untrimmed temporal video understanding while adapting the intermediate layers for TAL. The chart shows FP error breakdown for top-10 ground truth (GT) predictions. For more details regarding the chart, we refer the readers to [2].

S3 Limitations, Negative Impact, and Future Work

To our best knowledge, we do not perceive a potential negative impact that is specific to our proposed method. While LoSA’s memory-efficient design allows to leverage billion-parameter-plus models like VideoMAEv2 (ViT-g) for end-to-end TAL, the memory requirement is still linearly dependent (asymptotically) on the number of frames, frame resolution, and model size to a certain degree. In future, we can explore reducing the memory usage to sub-linear while continuing to improve performance as we leverage larger foundation models. Further interesting directions include extending to end-to-end spatio-temporal localization, end-to-end video object segmentation, end-to-end video grounding, and other multi-modal video understanding tasks involving audio, text, and other modalities.

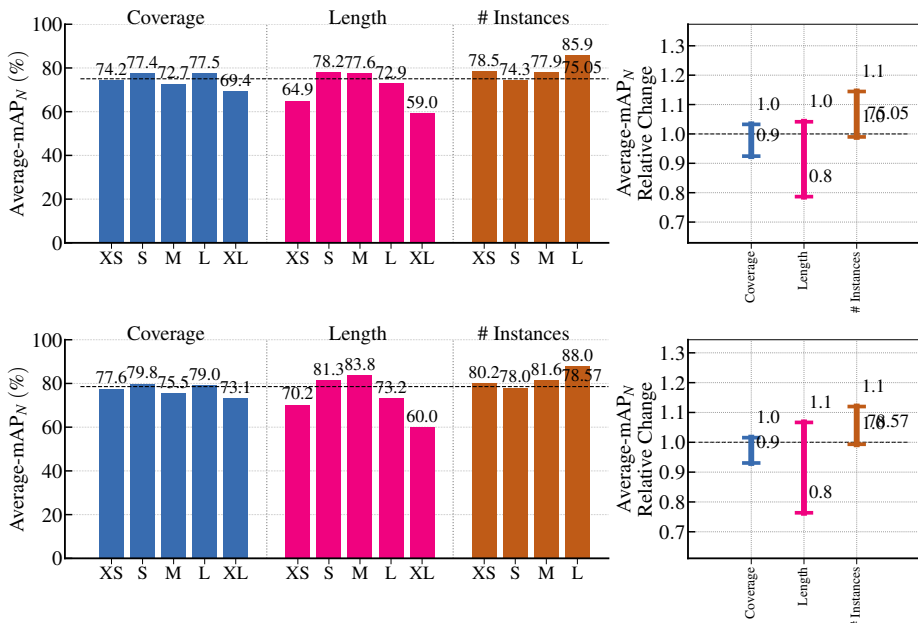


Fig. S3: Sensitivity analysis on THUMOS-14 using [2]. mAP_N denotes normalized mAP at $tIoU=0.5$ with N average ground truth segments per class. Top: LoSA w/o Long-Short-Adapter. Bottom: LoSA (ours). Performance for both XS and XL improves significantly with our method LoSA (bottom) compared to the baseline, LoSA w/o Long-Short-range Adapter (top).

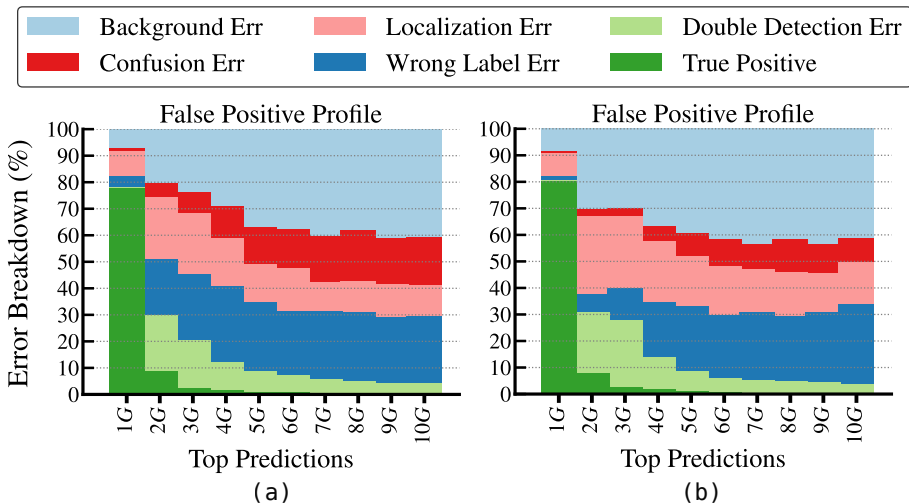


Fig. S4: False positive (FP) profiling on THUMOS-14 using [2]. FP error breakdown for top-10 ground-truth (GT) predictions comparing (a) LoSA w/o Long-Short-range Adapter and (b) LoSA (ours). Wrong label prediction error significantly drops with LoSA compared to LoSA w/o Long-Short-range Adapter.

References

1. Alwassel, H., Giancola, S., Ghanem, B.: Tsp: Temporally-sensitive pretraining of video encoders for localization tasks. In: Proceedings of the IEEE/CVF International Conference on Computer Vision. pp. 3173–3183 (2021) [4](#)
2. Alwassel, H., Heilbron, F.C., Escorcia, V., Ghanem, B.: Diagnosing error in temporal action detectors. In: Proceedings of the European conference on computer vision (ECCV). pp. 256–272 (2018) [19](#), [20](#)
3. Bai, Y., Wang, Y., Tong, Y., Yang, Y., Liu, Q., Liu, J.: Boundary content graph neural network for temporal action proposal generation. In: Computer Vision–ECCV 2020: 16th European Conference, Glasgow, UK, August 23–28, 2020, Proceedings, Part XXVIII 16. Springer (2020) [4](#)
4. Brown, T., Mann, B., Ryder, N., Subbiah, M., Kaplan, J.D., Dhariwal, P., Neelakantan, A., Shyam, P., Sastry, G., Askell, A., et al.: Language models are few-shot learners. *Advances in neural information processing systems* **33**, 1877–1901 (2020) [5](#)
5. Caba Heilbron, F., Escorcia, V., Ghanem, B., Carlos Niebles, J.: Activitynet: A large-scale video benchmark for human activity understanding. In: Proceedings of the IEEE conference on computer vision and pattern recognition. pp. 961–970 (2015) [9](#)
6. Carreira, J., Noland, E., Banki-Horvath, A., Hillier, C., Zisserman, A.: A short note about kinetics-600. *arXiv preprint arXiv:1808.01340* (2018) [1](#)
7. Carreira, J., Zisserman, A.: Quo vadis, action recognition? a new model and the kinetics dataset. In: proceedings of the IEEE Conference on Computer Vision and Pattern Recognition. pp. 6299–6308 (2017) [4](#)
8. Cheng, F., Bertasius, G.: Tallformer: Temporal action localization with a long-memory transformer. In: European Conference on Computer Vision. pp. 503–521. Springer (2022) [3](#), [4](#), [11](#)
9. Cheng, F., Xu, M., Xiong, Y., Chen, H., Li, X., Li, W., Xia, W.: Stochastic back-propagation: A memory efficient strategy for training video models. In: Proceedings of the IEEE/CVF Conference on Computer Vision and Pattern Recognition. pp. 8301–8310 (2022) [3](#), [4](#)
10. Cubuk, E.D., Zoph, B., Mane, D., Vasudevan, V., Le, Q.V.: Autoaugment: Learning augmentation strategies from data. In: Proceedings of the IEEE/CVF conference on computer vision and pattern recognition. pp. 113–123 (2019) [9](#)
11. Diao, H., Wan, B., Zhang, Y., Jia, X., Lu, H., Chen, L.: Unipt: Universal parallel tuning for transfer learning with efficient parameter and memory. *arXiv preprint arXiv:2308.14316* (2023) [5](#), [10](#)
12. Dosovitskiy, A., Beyer, L., Kolesnikov, A., Weissenborn, D., Zhai, X., Unterthiner, T., Dehghani, M., Minderer, M., Heigold, G., Gelly, S., et al.: An image is worth 16x16 words: Transformers for image recognition at scale. In: International Conference on Learning Representations (2020) [4](#)
13. Feichtenhofer, C., Fan, H., Malik, J., He, K.: Slowfast networks for video recognition. In: Proceedings of the IEEE/CVF international conference on computer vision. pp. 6202–6211 (2019) [4](#), [9](#)
14. Gong, G., Zheng, L., Mu, Y.: Scale matters: Temporal scale aggregation network for precise action localization in untrimmed videos. In: 2020 IEEE International Conference on Multimedia and Expo (ICME). pp. 1–6. IEEE (2020) [4](#)
15. He, K., Zhang, X., Ren, S., Sun, J.: Deep residual learning for image recognition. In: Proceedings of the IEEE conference on computer vision and pattern recognition. pp. 770–778 (2016) [4](#)

16. Houlby, N., Giurghi, A., Jastrzebski, S., Morrone, B., De Laroussilhe, Q., Gesmundo, A., Attariyan, M., Gelly, S.: Parameter-efficient transfer learning for nlp. In: International Conference on Machine Learning. pp. 2790–2799. PMLR (2019) [3](#), [5](#)
17. Hu, E.J., Wallis, P., Allen-Zhu, Z., Li, Y., Wang, S., Wang, L., Chen, W., et al.: Lora: Low-rank adaptation of large language models. In: International Conference on Learning Representations (2021) [3](#), [5](#)
18. Idrees, H., Zamir, A.R., Jiang, Y.G., Gorban, A., Laptev, I., Sukthankar, R., Shah, M.: The thumos challenge on action recognition for videos “in the wild”. *Computer Vision and Image Understanding* **155**, 1–23 (2017) [9](#)
19. Krizhevsky, A., Sutskever, I., Hinton, G.E.: Imagenet classification with deep convolutional neural networks. *Advances in neural information processing systems* **25** (2012) [9](#)
20. Lin, C., Xu, C., Luo, D., Wang, Y., Tai, Y., Wang, C., Li, J., Huang, F., Fu, Y.: Learning salient boundary feature for anchor-free temporal action localization. In: Proceedings of the IEEE/CVF Conference on Computer Vision and Pattern Recognition. pp. 3320–3329 (2021) [1](#), [4](#), [9](#), [11](#)
21. Lin, T., Liu, X., Li, X., Ding, E., Wen, S.: Bmn: Boundary-matching network for temporal action proposal generation. In: Proceedings of the IEEE/CVF international conference on computer vision. pp. 3889–3898 (2019) [4](#)
22. Lin, T., Zhao, X., Su, H., Wang, C., Yang, M.: Bsn: Boundary sensitive network for temporal action proposal generation. In: Proceedings of the European conference on computer vision (ECCV). pp. 3–19 (2018) [4](#)
23. Liu, X., Bai, S., Bai, X.: An empirical study of end-to-end temporal action detection. In: Proceedings of the IEEE/CVF Conference on Computer Vision and Pattern Recognition. pp. 20010–20019 (2022) [3](#), [4](#), [11](#)
24. Liu, X., Wang, Q., Hu, Y., Tang, X., Zhang, S., Bai, S., Bai, X.: End-to-end temporal action detection with transformer. *IEEE Transactions on Image Processing* (2022) [4](#), [11](#)
25. Liu, Z., Ning, J., Cao, Y., Wei, Y., Zhang, Z., Lin, S., Hu, H.: Video swin transformer. In: Proceedings of the IEEE/CVF conference on computer vision and pattern recognition. pp. 3202–3211 (2022) [11](#)
26. Loshchilov, I., Hutter, F.: Decoupled weight decay regularization. In: International Conference on Learning Representations (2018) [9](#)
27. Pan, J., Lin, Z., Zhu, X., Shao, J., Li, H.: St-adapter: Parameter-efficient image-to-video transfer learning. *Advances in Neural Information Processing Systems* **35**, 26462–26477 (2022) [10](#)
28. Rizve, M.N., Mittal, G., Yu, Y., Hall, M., Sajeev, S., Shah, M., Chen, M.: Pivotal: Prior-driven supervision for weakly-supervised temporal action localization. In: Proceedings of the IEEE/CVF Conference on Computer Vision and Pattern Recognition. pp. 22992–23002 (2023) [1](#)
29. Shi, D., Zhong, Y., Cao, Q., Ma, L., Li, J., Tao, D.: Tridet: Temporal action detection with relative boundary modeling. In: Proceedings of the IEEE/CVF Conference on Computer Vision and Pattern Recognition. pp. 18857–18866 (2023) [2](#), [4](#), [11](#)
30. Sung, Y.L., Cho, J., Bansal, M.: Lst: Ladder side-tuning for parameter and memory efficient transfer learning. *Advances in Neural Information Processing Systems* **35**, 12991–13005 (2022) [3](#), [5](#)
31. Tang, T.N., Kim, K., Sohn, K.: Temporalmixer: Maximize temporal context with only max pooling for temporal action localization. *arXiv preprint arXiv:2303.09055* (2023) [2](#), [4](#)

32. Touvron, H., Martin, L., Stone, K., Albert, P., Almahairi, A., Babaei, Y., Bashlykov, N., Batra, S., Bhargava, P., Bhosale, S., et al.: Llama 2: Open foundation and fine-tuned chat models. arXiv preprint arXiv:2307.09288 (2023) [5](#)
33. Vaswani, A., Shazeer, N., Parmar, N., Uszkoreit, J., Jones, L., Gomez, A.N., Kaiser, Ł., Polosukhin, I.: Attention is all you need. *Advances in neural information processing systems* **30** (2017) [9](#)
34. Wang, L., Huang, B., Zhao, Z., Tong, Z., He, Y., Wang, Y., Wang, Y., Qiao, Y.: Videomae v2: Scaling video masked autoencoders with dual masking. In: *Proceedings of the IEEE/CVF Conference on Computer Vision and Pattern Recognition*. pp. 14549–14560 (2023) [1](#), [2](#), [4](#), [9](#), [11](#)
35. Wang, L., Xiong, Y., Wang, Z., Qiao, Y., Lin, D., Tang, X., Van Gool, L.: Temporal segment networks: Towards good practices for deep action recognition. In: *European conference on computer vision*. pp. 20–36. Springer (2016) [4](#)
36. Wang, Y., Li, K., Li, Y., He, Y., Huang, B., Zhao, Z., Zhang, H., Xu, J., Liu, Y., Wang, Z., et al.: Internvideo: General video foundation models via generative and discriminative learning. arXiv preprint arXiv:2212.03191 (2022) [2](#), [4](#)
37. Wu, P., Liu, J., Shi, Y., Sun, Y., Shao, F., Wu, Z., Yang, Z.: Not only look, but also listen: Learning multimodal violence detection under weak supervision. In: *Computer Vision—ECCV 2020: 16th European Conference, Glasgow, UK, August 23–28, 2020, Proceedings, Part XXX 16*. pp. 322–339. Springer (2020) [1](#)
38. Xu, M., Pérez-Rúa, J.M., Escorcia, V., Martinez, B., Zhu, X., Zhang, L., Ghanem, B., Xiang, T.: Boundary-sensitive pre-training for temporal localization in videos. In: *Proceedings of the IEEE/CVF International Conference on Computer Vision*. pp. 7220–7230 (2021) [2](#)
39. Xu, M., Zhao, C., Rojas, D.S., Thabet, A., Ghanem, B.: G-tad: Sub-graph localization for temporal action detection. In: *Proceedings of the IEEE/CVF conference on computer vision and pattern recognition*. pp. 10156–10165 (2020) [1](#), [4](#), [11](#)
40. Yang, T., Zhu, Y., Xie, Y., Zhang, A., Chen, C., Li, M.: Aim: Adapting image models for efficient video action recognition. In: *The Eleventh International Conference on Learning Representations* (2022) [5](#), [10](#)
41. Yin, D., Han, X., Li, B., Feng, H., Bai, J.: Parameter-efficient is not sufficient: Exploring parameter, memory, and time efficient adapter tuning for dense predictions. arXiv preprint arXiv:2306.09729 (2023) [5](#)
42. Yu, B.X., Chang, J., Wang, H., Liu, L., Wang, S., Wang, Z., Lin, J., Xie, L., Li, H., Lin, Z., et al.: Visual tuning. arXiv preprint arXiv:2305.06061 (2023) [3](#)
43. Zhai, X., Kolesnikov, A., Houlsby, N., Beyer, L.: Scaling vision transformers. In: *Proceedings of the IEEE/CVF Conference on Computer Vision and Pattern Recognition*. pp. 12104–12113 (2022) [2](#)
44. Zhang, C.L., Wu, J., Li, Y.: Actionformer: Localizing moments of actions with transformers. In: *European Conference on Computer Vision*. pp. 492–510. Springer (2022) [1](#), [2](#), [4](#), [9](#), [11](#)
45. Zhao, C., Liu, S., Mangalam, K., Ghanem, B.: Re2tal: Rewiring pretrained video backbones for reversible temporal action localization. In: *Proceedings of the IEEE/CVF Conference on Computer Vision and Pattern Recognition*. pp. 10637–10647 (2023) [3](#), [4](#), [11](#)
46. Zhao, P., Xie, L., Ju, C., Zhang, Y., Wang, Y., Tian, Q.: Bottom-up temporal action localization with mutual regularization. In: *Computer Vision—ECCV 2020: 16th European Conference, Glasgow, UK, August 23–28, 2020, Proceedings, Part VIII 16*. pp. 539–555. Springer (2020) [4](#)